Geometrical dispersion of dielectric and optic axes in a monoclinic crystal

W. Lang

Sektion Physik der LM-Universität, München, Lehrst. J. Brandmueller, 8000 München 40, Federal Republic of Germany

R. Claus

Universidad Autónoma de Puebla, Instituto de Ciencias, Departamento de Fisica, Adpo. Postal J-48 Puebla, Puebla, México

Angular dependences of coupled B-phonon frequencies with wave vectors varying perpendicularly to the symmetry axis in monoclinic $Li_2SO_4 \cdot H_2O$ have been recorded by light scattering. A numerical fit allows the determination of B(TO) frequencies and mode strength parameters. With the use of these, the A(TO) and A(LO) frequencies directional dispersion of dielectric and optic axes could be calculated for the entire infrared region from 250 to 3800 cm^{-1}.

The positions of the principal dielectric axes in monoclinic and triclinic crystals are not related to any specific crystallographic direction. In particular the orientation varies with frequency. Whereas in triclinic systems the orthogonal dielectric tripod is free to move in space, in monoclinic materials the orientation at least of one of its axes coincides with the twofold symmetry axis, or is perpendicular to the mirror plane for all frequencies.[1] Straightforward optical measurements concerning the dispersion of dielectric and optic axes in the infrared (IR) by means of modified methods from the visible turned out to be too extensive and not very successful because of severe difficulties that absorption causes. Previous corresponding experiments therefore do not go further than to verify that the dispersion effects in question principally exist.[2,3] Numerical calculations, on the other hand, require all components of the dielectric tensor to be known explicitly as a function of frequency. We show in the following that light scattering experiments concerning transverse and longitudinal A phonons and coupled oblique B phonons with wave vectors varying in the xz-plane perpendicularly to the twofold symmetry axis y in monoclinic $Li_2SO_4 \cdot H_2O$ provide the full information necessary to write $\epsilon_{ij}(\omega)$ explicitly. As a result we present for the first time the entire geometrical dispersion phenomena of dielectric and optic axes for one of the lowest two symmetry crystal classes and the infrared spectral region.

The interrelation between polariton dispersion and crystal optics in monoclinic and triclinic systems was first discussed in 1978.[4,5] It could be shown that in the long-wave limit, i.e., $k \approx 10^5$ cm^{-1}, the polariton dispersion relation reduces to $\vec{s} \cdot \vec{\epsilon} \cdot \vec{s} = 0$ and when restricted to, e.g., the xz plane of the laboratory system

$$\epsilon_{xx}(\omega) s_x^2 + \epsilon_{zz}(\omega) s_z^2 + 2\epsilon_{xz}(\omega) s_x s_z = 0 \quad . \tag{1}$$

$\vec{s}$ is the normal wave vector. In the case of the monoclinic crystal under discussion Eq. (1) represents the dispersion relation of coupled B phonons providing their frequencies as a function of varying $\vec{s}$.

The elements of the dielectric tensor in the infrared, on the other hand, become in their undamped forms

$$\epsilon_{xx}(\omega) = \epsilon_{xx}^{\infty} + \sum_i \frac{1}{\epsilon_0} B_{xi}^2 (\omega_{Ti}^2 - \omega^2)^{-1} \quad , \tag{2a}$$

$$\epsilon_{yy}(\omega) = \epsilon_{yy}^{\infty} + \sum_j \frac{1}{\epsilon_0} B_{yj}^2 (\omega_{Tj}^2 - \omega^2)^{-1} \quad , \tag{2b}$$

$$\epsilon_{zz}(\omega) = \epsilon_{zz}^{\infty} + \sum_i \frac{1}{\epsilon_0} B_{zi}^2 (\omega_{Ti}^2 - \omega^2)^{-1} \quad , \tag{2c}$$

$$\epsilon_{xz}(\omega) = \epsilon_{zx}(\omega) = \sum_i \frac{1}{\epsilon_0} B_{xi} B_{zi} (\omega_{Ti}^2 - \omega^2)^{-1} \quad . \tag{2d}$$

For $\omega \to \infty$ we find $\epsilon_{xz} = 0$. The tensor thus is diagonalized with approximately constant elements ϵ_{xx}^{∞}, ϵ_{yy}^{∞}, and ϵ_{zz}^{∞} in the band gap. The principal dielectric axes determined in this way are chosen as the laboratory system. It varies owing to the uncertainty in their choice by $< 3°$. When defining θ as the angle between the wave vector of B phonons and the x axis of this system, i.e., $s_x = \cos\theta$ and $s_z = \sin\theta$, Eq. (1) can be rewritten

$$\epsilon_{xx}^{\infty} \cos^2\theta + \epsilon_{zz}^{\infty} \sin^2\theta$$
$$+ \sum_i \frac{1}{\epsilon_0} (B_{xi}\cos\theta + B_{zi}\sin^2\theta)^2 (\omega_{Ti}^2 - \omega^2)^{-1} = 0 \quad . \tag{3}$$

A numerical fit of the B-phonons angular dispersion by (3) provides the transverse eigenfrequencies ω_{Ti} and mode strength parameters B_{xi} and B_{zi}. Basically every dispersion branch (i) is supposed to determine one of each group of parameters and since each branch in average is recorded by a larger number of experimental data points Eq. (3) forms a profound

basis to calculate the parameters in question.

The poles and zeros of $\epsilon_{yy}(\omega)$ are found for the TO- and LO-frequencies of A modes in the usual way. If these are recorded also the B_{yj}^2 in (2b) are known.

Angular dispersion of the dielectric axes as a function of ω is derived by transforming the ϵ tensor to diagonal form. This condition leads to

$$tg2\phi(\omega) = 2\epsilon_{xz}(\omega)/[\epsilon_{zz}(\omega) - \epsilon_{xx}(\omega)] \quad . \qquad (4)$$

ϕ is the angle between, e.g., the $\epsilon_{xx}(\omega)$ and the ϵ_{xx}^{∞} direction and y the rotational axis.

The dispersion of the optic axes, on the other hand, is given by

$$\sin^2\psi(\omega) = \frac{\epsilon_\gamma(\omega)[\epsilon_\beta(\omega) - \epsilon_\alpha(\omega)]}{\epsilon_\beta(\omega)[\epsilon_\gamma(\omega) - \epsilon_\alpha(\omega)]} \quad , \qquad (5)$$

see, e.g., Ref. 6. ϵ_α, ϵ_β, and ϵ_γ are elements of the diagonalized ϵ tensor. When $\epsilon_\alpha < \epsilon_\beta < \epsilon_\gamma$, the two optic axes are located in the $\alpha\gamma$ plane forming an angle of 2ψ. ψ itself is measured from the γ axis.

Single-crystalline $Li_2SO_4 \cdot H_2O$ belongs to the space group $p2_1(C_2^2)$, see Ref. 7. There are two formula units per unit cell. Factor group analysis provides $\Gamma(p2_1) = 29A + 28B$. Since there is no inversion center all phonons are simultaneously IR and Raman active. Our spectra were recorded by means of a cylindrical sample and in backward scattering geometries. The values used for the high-frequency dielectric constants in the band gap were

$$\epsilon_{xx}^{\infty} = 2.15; \quad \epsilon_{yy}^{\infty} = 2.21; \quad \epsilon_{zz}^{\infty} = 2.18 \quad .$$

Table I summarizes phonon frequencies and mode strength parameters. For $\omega < 250$ cm^{-1} all B phonons remained independent of θ within the experimental error. Similarly no TO-LO splittings of A modes could be recorded. We therefore exclude this region from further calculations. This is justified also because some of the signals might easily correspond to difference frequencies whereas the Raman scattering intensities by fundamentals could be too weak. In the region $\omega > 300$ cm^{-1} both TO-LO splittings of A modes and oblique B-phonon directional dispersion were observed systematically. The best numerical fit of the latter by Eq. (3) for 14 dispersion branches is shown in Fig. 1. The minima and maxima of the curves indicate the frequencies of purely transversal and longitudinal B phonons, respectively, and the wave-vector directions related to these. They are not fixed any longer to crystallographic directions as in all higher symmetry crystals.[8-11]

The left- and right-hand diagrams in Fig. 2, respectively, show the dispersion of dielectric axes in the xz

TABLE I. Phonon frequencies and their mode-strength parameters. Frequencies are in cm^{-1}; mode strength parameters are in sec^{-1}.

A modes ω		B modes ω		
45		36		
53		40		
60		54		
77		79		
84		91		
96		103		
109		135		
122		159		
147		194		
174		219		
208		232		
233				
ω_T	ω_L	ω_T	$\epsilon_0^{-1/2}B_x$	$\epsilon_0^{-1/2}B_z$
315	322	363	−228	61
359	387	395	−152	96
395	405	417	294	157
413	433	458	−49	202
466	488	482	73	106
488.5	508	548	−173	276
615	636	610	$\cdots$	$\cdots$
641	660	628	42	166
1010	1010	641	−142	78
1102	1148	1098	−462	201
1150	1173	1121	−103	165
1180	1191	1179	220	407
1615	1615	1300	$\cdots$	$\cdots$
3208	$\cdots$	1610	−8	224
3440	3443	3456	−256	463
3537	$\cdots$	3508	−648	201
3620	$\cdots$	3580	$\cdots$	$\cdots$

plane $\omega = \omega(\phi)$ [Eq. (4)] and that of the optic axes $\omega = \omega(\psi)$ [Eq. (5)]. The spectral range covers all pronounced resonances in the IR. The optic axes generally are located in the plane determined by the minimum and maximum element of the diagonalized ϵ tensor. The letter combinations of type zxy, ... to the right indicate the sequences $\epsilon_z < \epsilon_x < \epsilon_y$ in different regions of transparency. For $\omega = 2980$ cm^{-1} the x and z axes are interchanged so there is a jump in ϕ from $-45°$ to $+45°$. Since damping was ignored in our calculations the horizontal dashed lines "sharply" distinguish regions of transparency and reflections (reststrahlen bands). This implies still some simplification.

Studies of dielectric and optic properties of monoclinic and triclinic crystals generally are supposed to be severely complicated by the fact that there is a
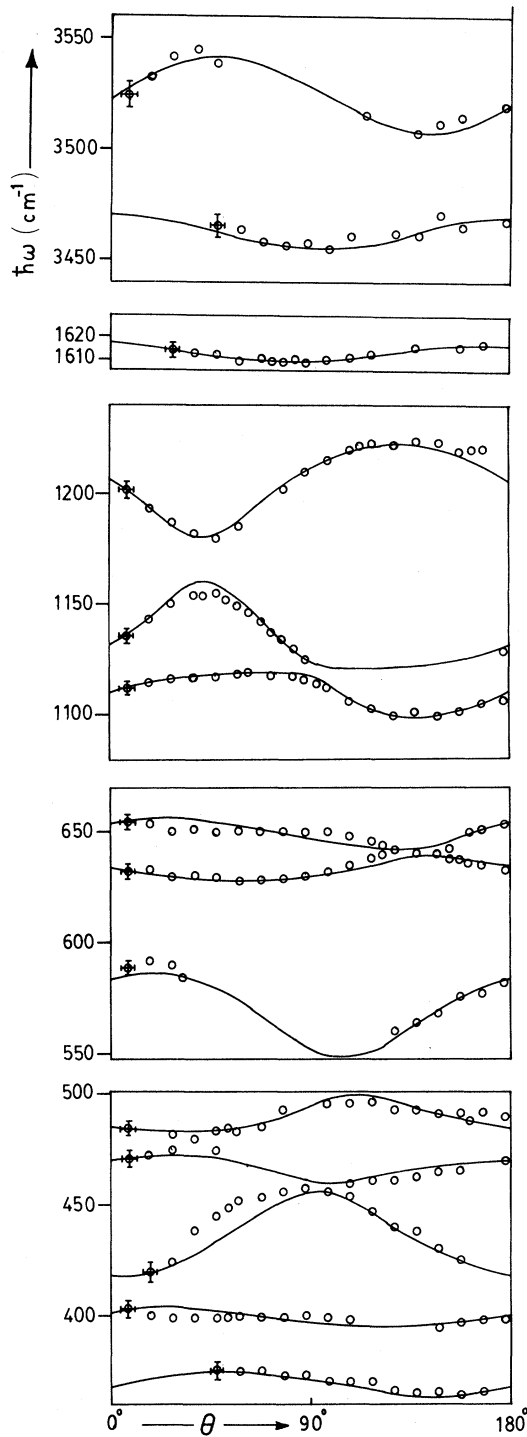
FIG. 1. Directional dispersion of coupled oblique B phonons with varying wave-vector directions perpendicular to the twofold symmetry axis in monoclinic $Li_2SO_4 \cdot H_2O$. θ is the angle between the phonon wave vector and the dielectric x axis of the laboratory system (see text).
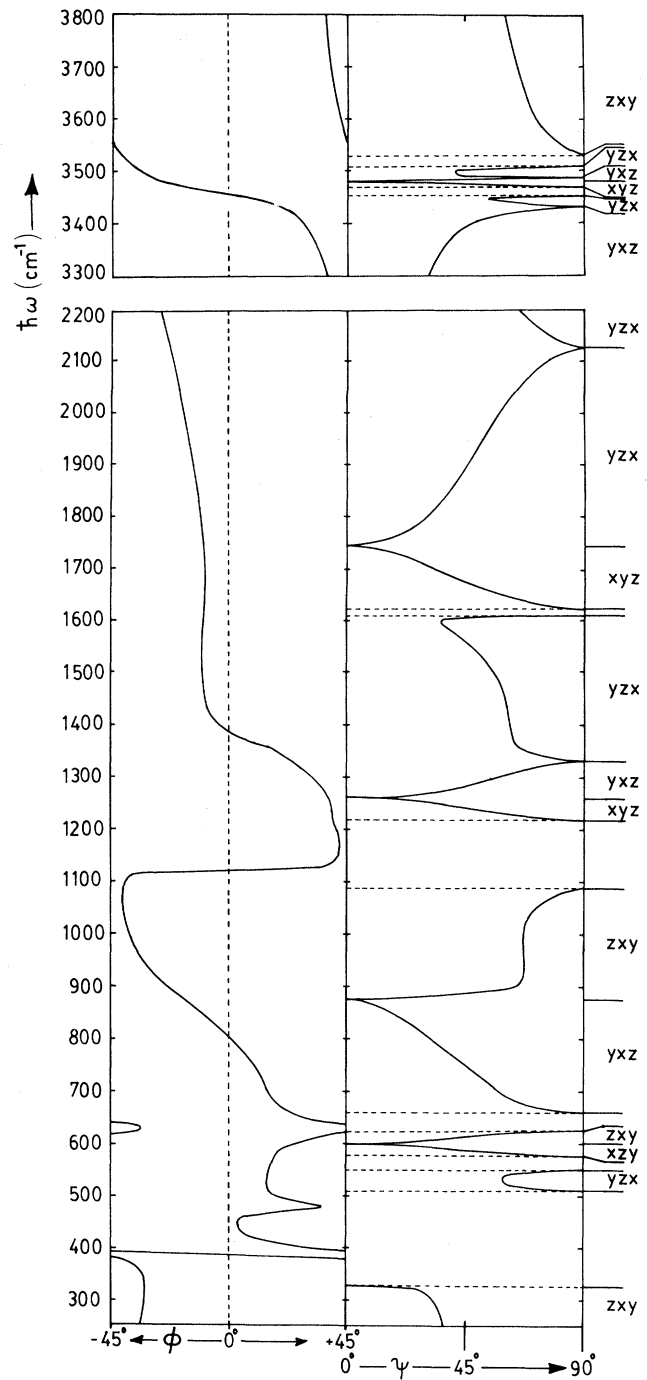
FIG. 2. Dispersion of dielectric and optic axes in monoclinic $Li_2SO_4 \cdot H_2O$, left and right diagram, respectively. ϕ indicates the deviation of the dielectric x axis from its position in the band gap. The two optical axes form an angle 2ψ and are located in the plane determined by the minimum and maximum element of the diagonalized ϵ tensor. The three letter combinations to the right indicate, e.g., $\epsilon_z < \epsilon_x < \epsilon_y$.

lack of an appropriate, orthogonal coordinate system. It has been shown above that the geometrical dispersion effects of optic and orthogonal dielectric axes in monoclinic crystals can be calculated in all detail on the basis of lattice dynamical data in particular concerning directional dispersion of oblique B phonons. The extension to triclinic systems requires corresponding measurements in three orthogonal planes only, see Ref. 12.

ACKNOWLEDGMENTS

[1]L. D. Landau and E. M. Lifschitz, in *Course of Theoretical Physics* (Pergamon, Oxford, 1960), Vol. 8, p. 324.

[2]H. Rubens, Z. Phys. 1, 11 (1920).

[3]E. Goens, Z. Phys. 6, 12 (1921).

[4]R. Claus, Phys. Status Solidi B 88, 683 (1978).

[5]R. Claus and G. Borstel, Phys. Status Solidi B 88, K123 (1978).

[6]G. Szivessy, in *Handbook of Physics* (Springer, Berlin, 1928), Vol. XX.

[7]G. E. Ziegler, Z. Kristallogr. Mineral 89, 456 (1934).

[8]S. M. Sharipo and J. D. Axe, Phys. Rev. B 6, 2420 (1972).

[9]J. F. Scott, Am. J. Phys. 39, 1360 (1971).

[10]C. M. Hartwig, E. Wiener-Avnear, J. Smit, and S. P. S. Porto, Phys. Rev. B 3, 2078 (1971).

[11]L. Graf, G. Schaack, and B. Unger, Phys. Status Solidi B 54, 261 (1972).

[12]R. Claus, Phys. Status Solidi B 100, 9 (1980).